

The Madden-Julian Oscillation in General Circulation Models

Kenneth R. Sperber¹, Julia M. Slingo²,
Peter M. Inness², Silvio Gualdi³, Wei Li⁴,
Peter J. Gleckler¹, Charles Doutriaux¹,
and the AMIP and CMIP Modelling Groups

¹Program for Climate Model Diagnosis and Intercomparison, Lawrence Livermore National Laboratory, P.O. Box 808, L-103, Livermore, CA 94550 USA ([Contact: sperber1@llnl.gov](mailto:sperber1@llnl.gov))

²NCAS Centre for Global Atmospheric Modelling, Dept. of Meteorology, University of Reading, P.O. Box 243, Reading RG6 6BB, England

³National Institute of Geophysics and Volcanology, Via Gobetti 101, 40129 Bologna, Italy

⁴LASG, Institute of Atmospheric Physics, P.O. Box 9804, Beijing 100029, China

ECMWF Workshop on “Simulation and Prediction of Intra-Seasonal
Variability with Emphasis on the MJO”
3-6 November 2003

This work was performed under the auspices of the U.S. Department of Energy by University of California, Lawrence Livermore National Laboratory under Contract W-7405-Eng-48.

Goals

-evaluate the ability of the AMIP and CMIP models to simulate the boreal winter

Madden-Julian Oscillation

- propagation

- mechanisms

- vertical structure

- role of air-sea interaction

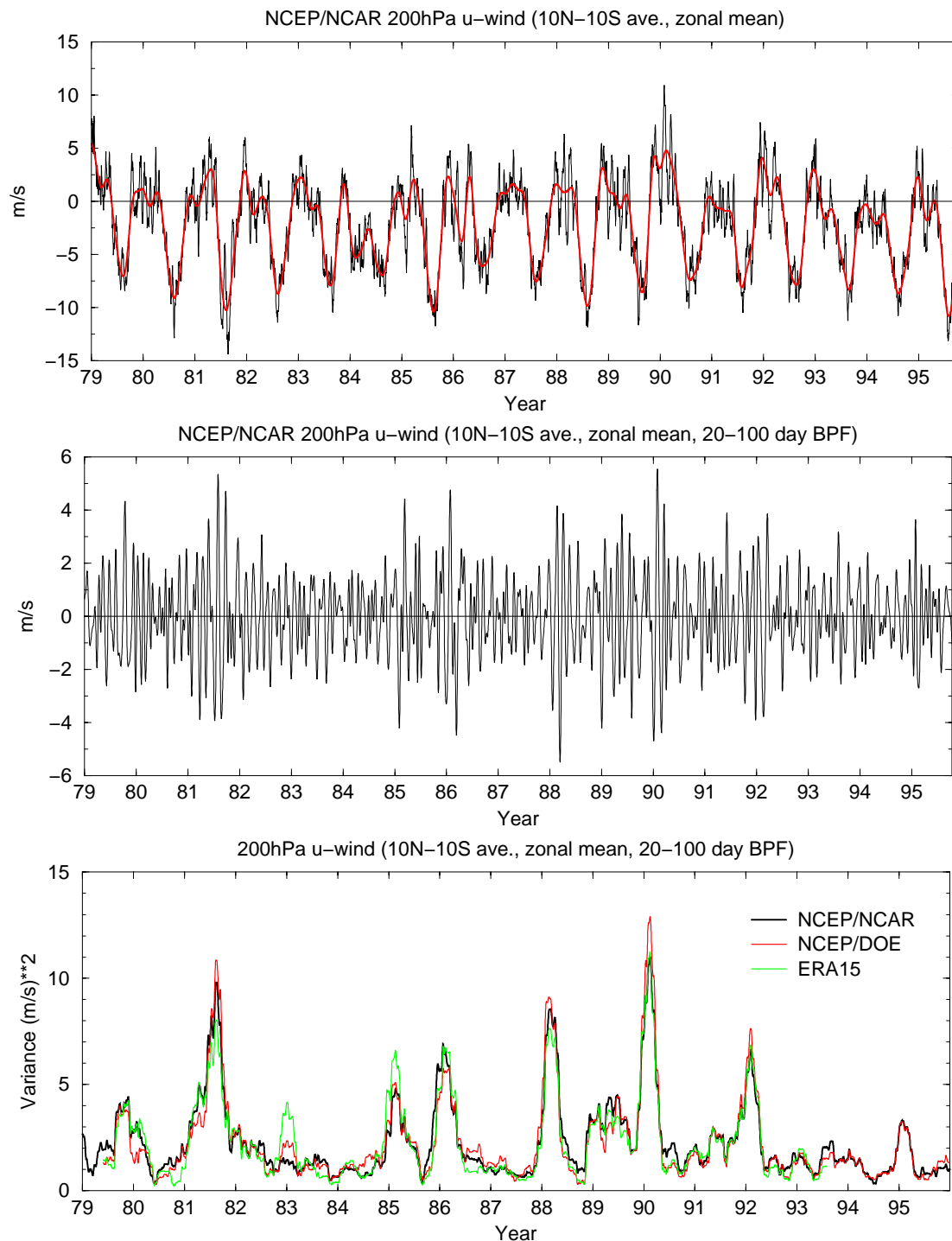
- relationship between mean state error and the MJO

Daily Data (November-March)

- NCEP-NCAR Reanalysis
 - CPC Merged Analysis of Precipitation (CMAP)
 - Advanced Very High Resolution Radiometer OLR
-
- 20 AMIP Models (1979/80-1994/95)
 - 9 Coupled Models (9-19 winters)

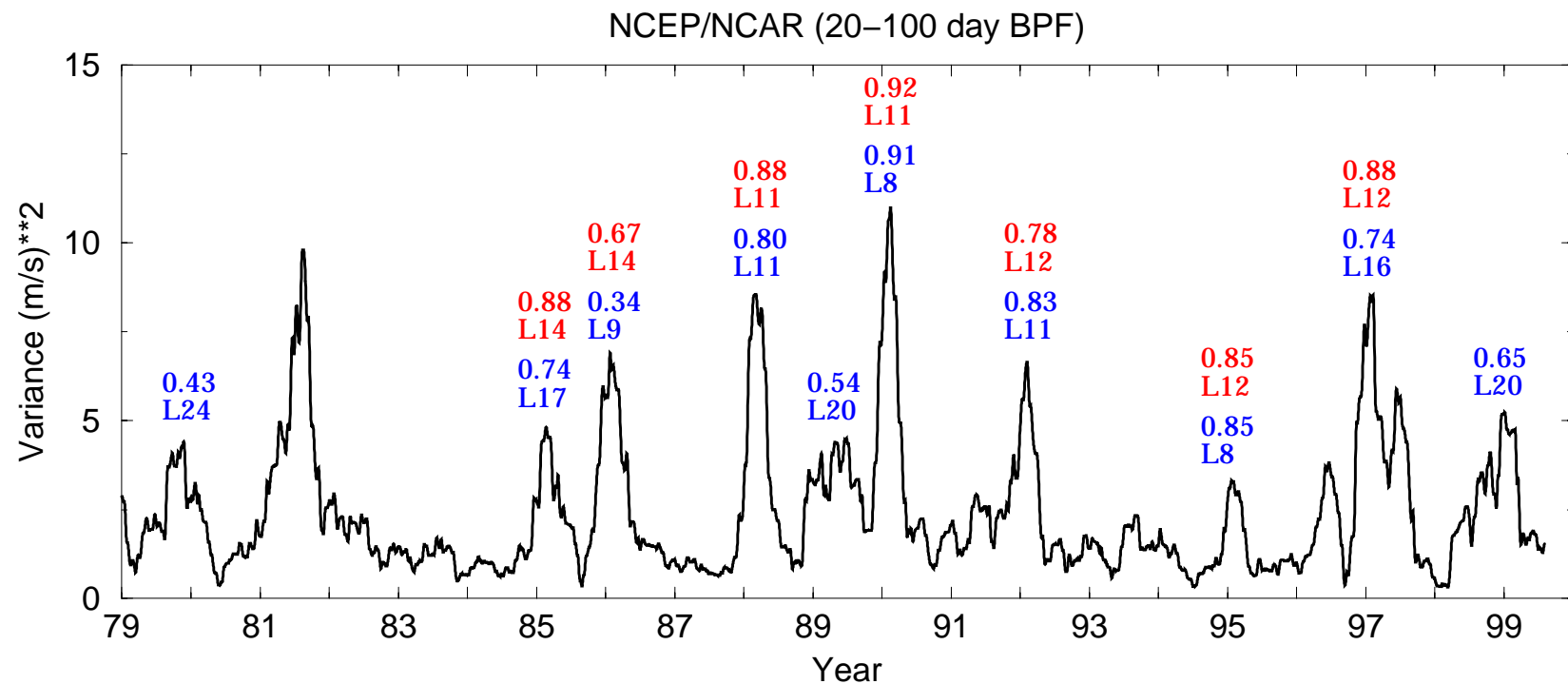
Analysis

- 1) MJO Index
 - intraseasonal variability of the 200hPa tropical zonal mean zonal wind
 - used to identify years of strong MJO variability
- 2) EOF analysis of 20-100 day bandpass filtered AVHRR OLR during years of strong MJO variability
 - isolate propagation characteristics of MJO convection
- 3) Project the 20-100 day bandpass filtered OLR from the observations (1979/80-1994/95) and models onto the observed EOF's to obtain PC's
- 4) For each model identify years when the simulated lead/lag behavior of the PC's is consistent with observations
- 5) For these years, linear regression of PC time series against 20-100 day bandpass filtered OLR, rainfall, winds etc. to evaluate observed/simulated spatio-temporal evolution of the MJO. All regressions have been scaled by a 1 standard deviation perturbation of the PC to return actual units



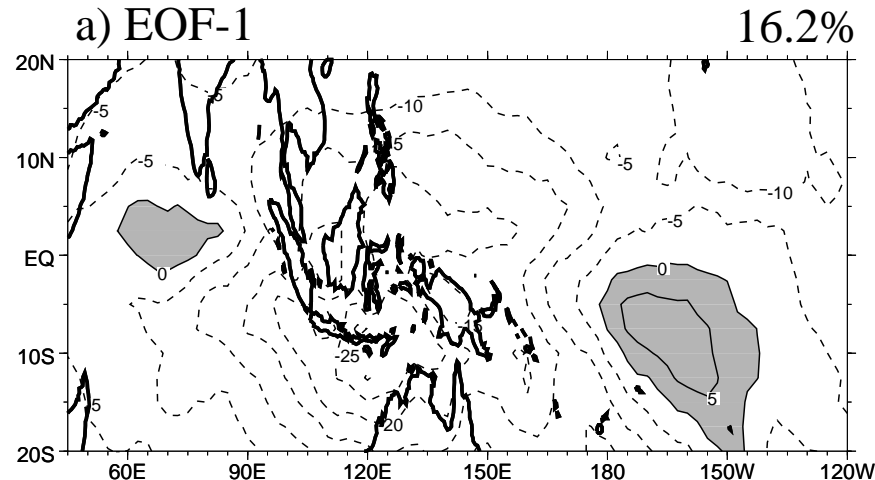
The 200hPa zonal mean zonal wind MJO index

Based on EOF analysis of 20-100 day filtered OLR, characteristics of the lead-lag relationship of the 2 leading PC's are also given, including the maximum positive correlation, and the time lag (L 'n'; days) at which it occurred. Blue (red) labelling is from the analysis of 10 (7) winters of data.

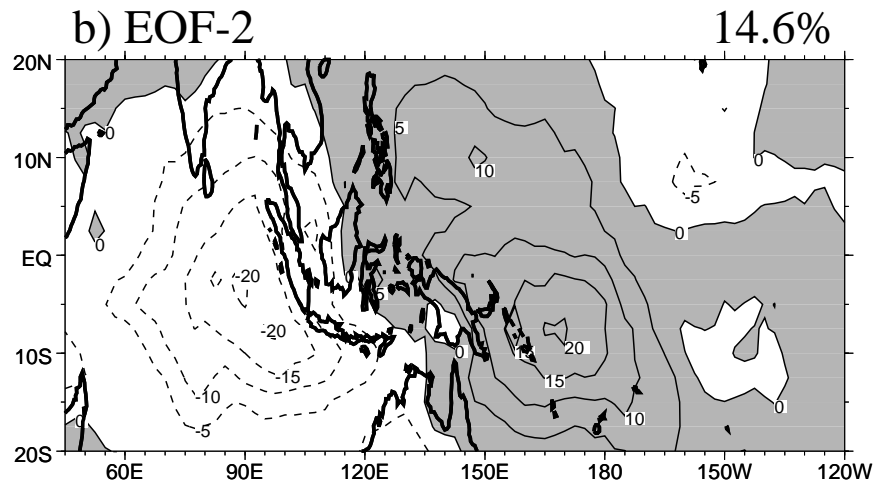


Characteristics of the two leading EOF's/PC's using seven winters of 20-100 day filtered OLR

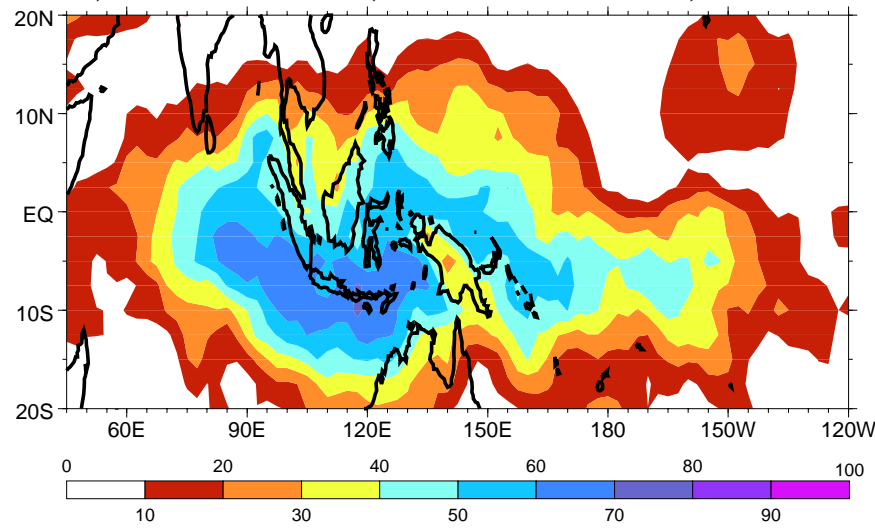
a) EOF-1



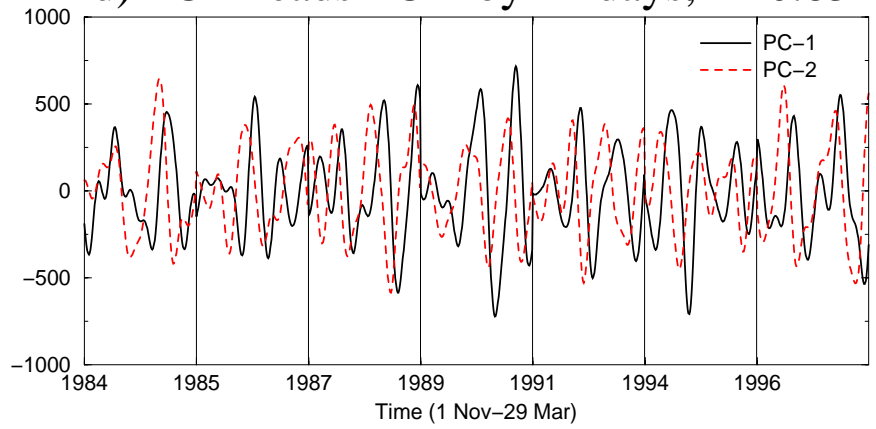
b) EOF-2



c) % Variance (EOF-1 + EOF-2)



d) PC-2 leads PC-1 by 12 days, R=0.83



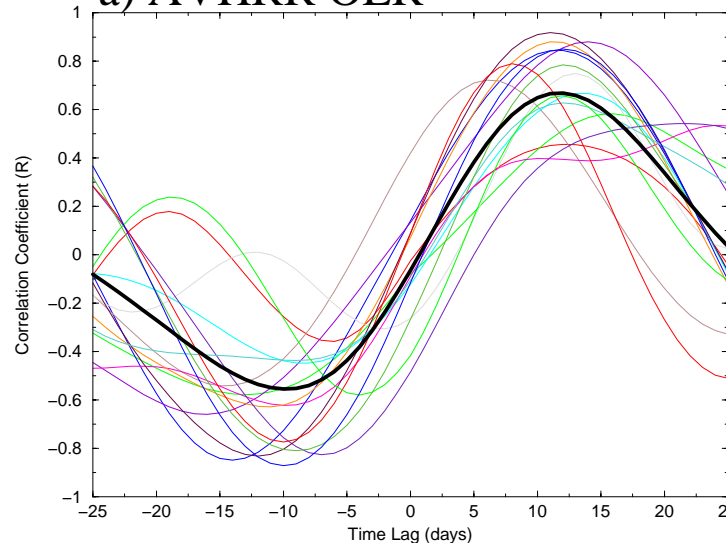
Lead-lag relationship between PC-1 and PC-2

-colored lines: individual winters

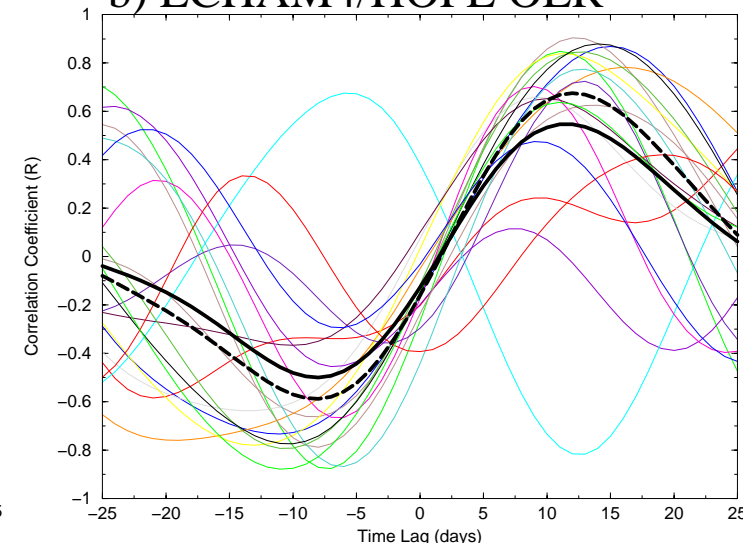
-thick solid black line: average over all winters

-thick dashed black line: average of winters in observed phase-space

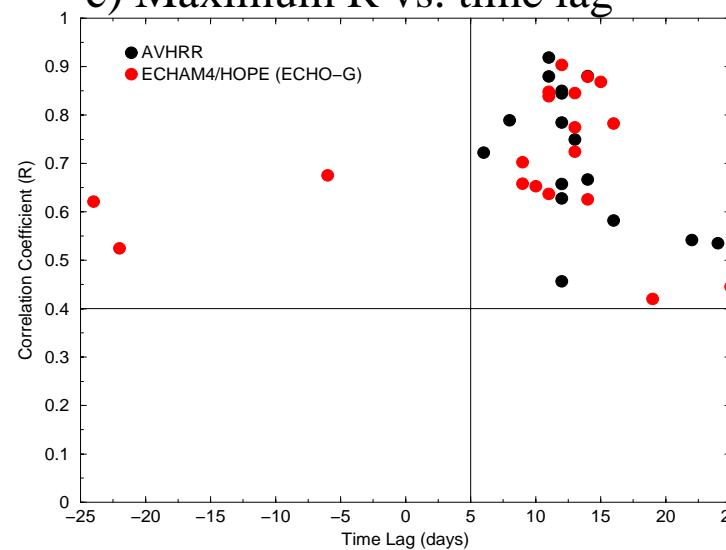
a) AVHRR OLR



b) ECHAM4/HOPE OLR

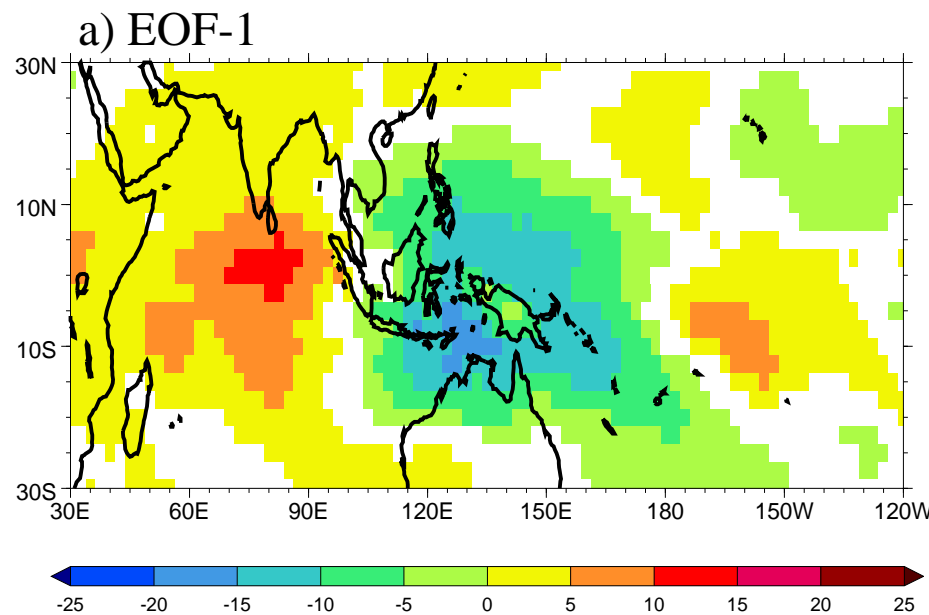


c) Maximum R vs. time lag

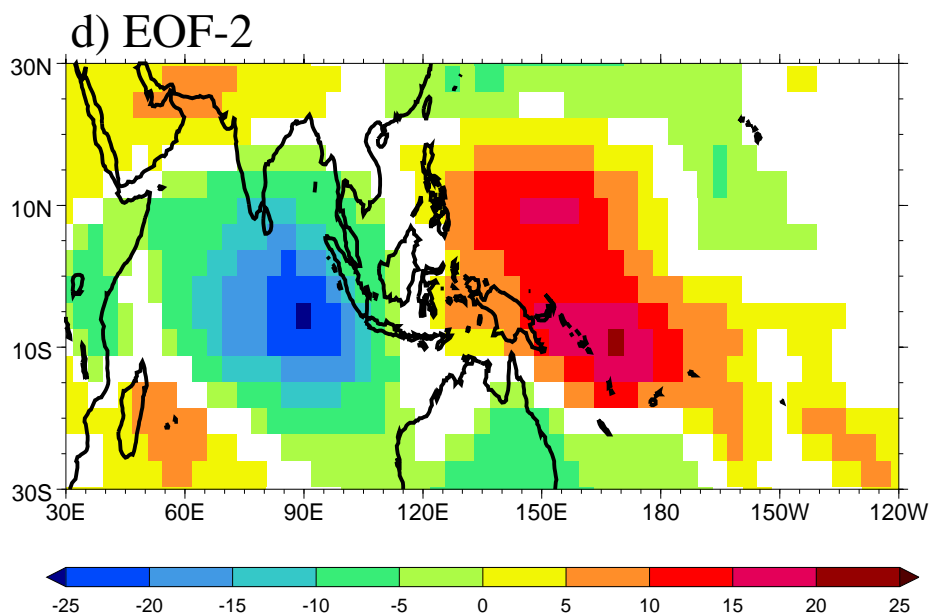
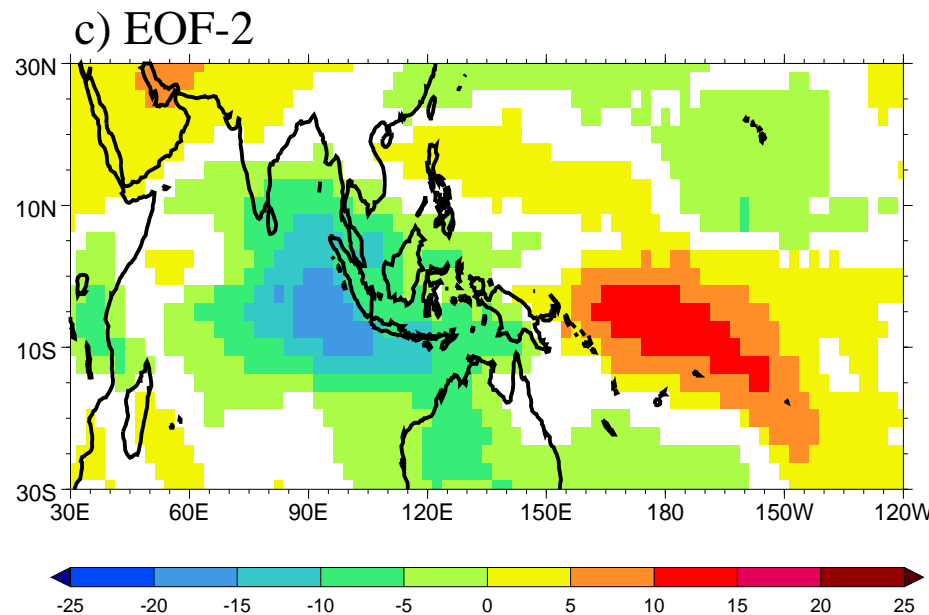
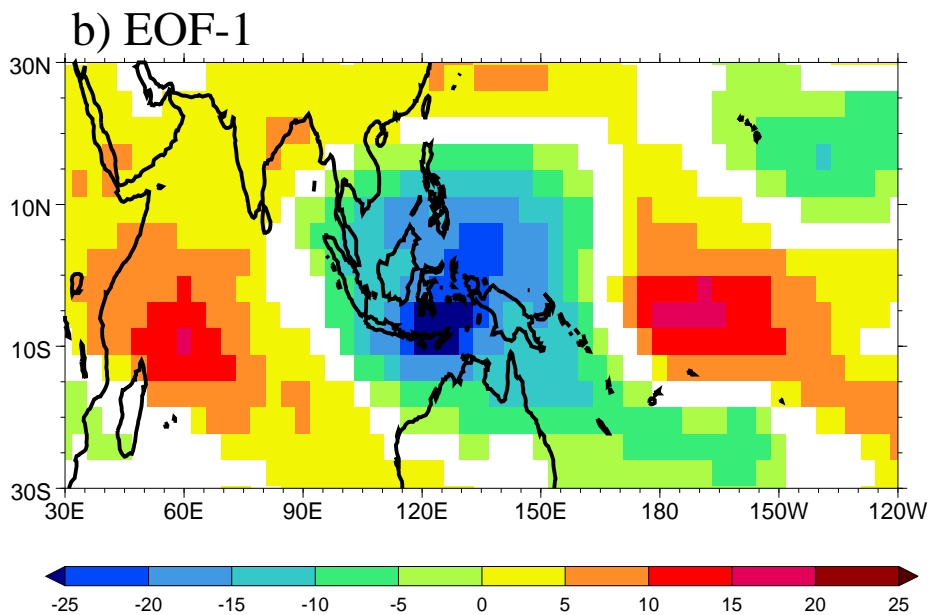


Lag 0 regression of PC-1 and PC-2 with filtered OLR

AVHRR OLR

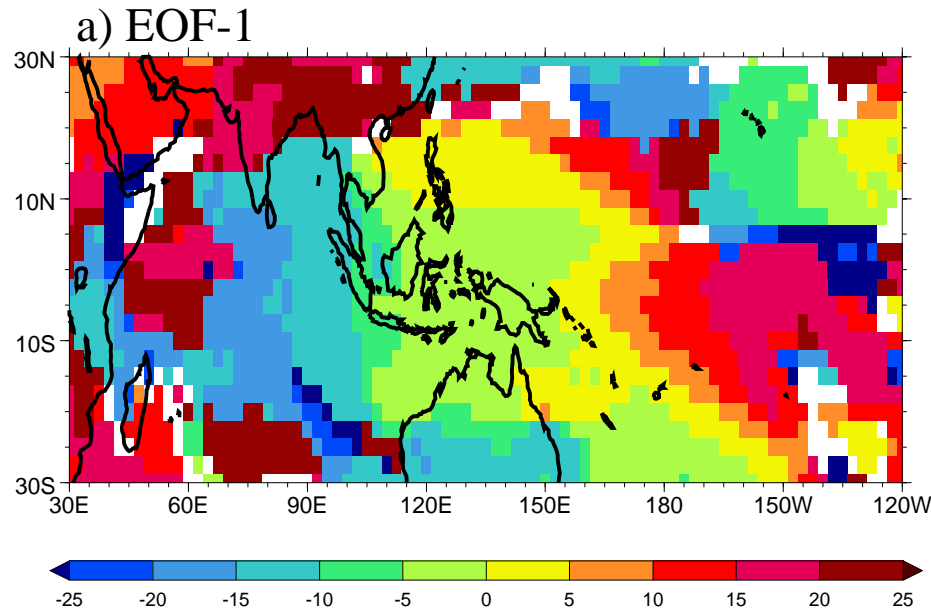


ECHAM4/HOPE

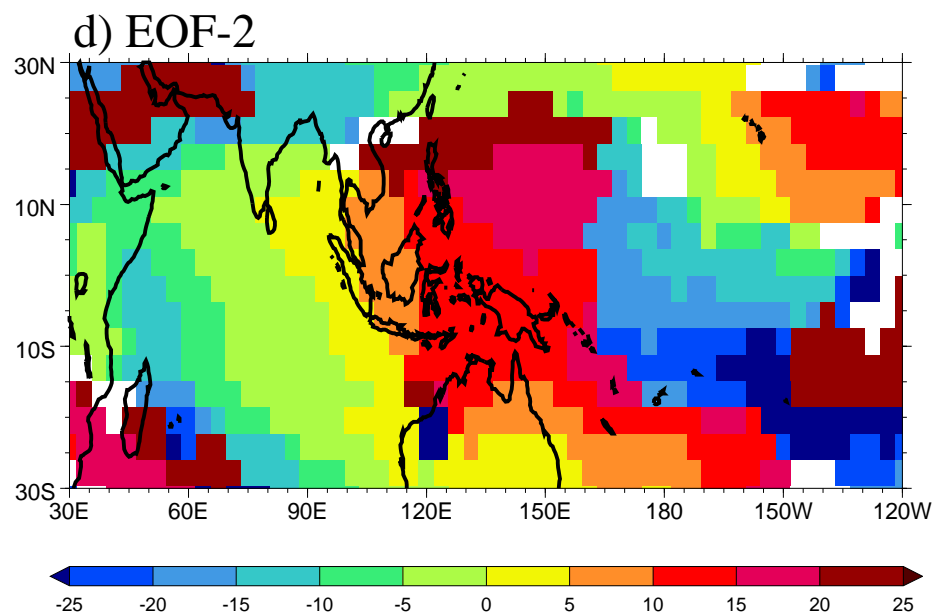
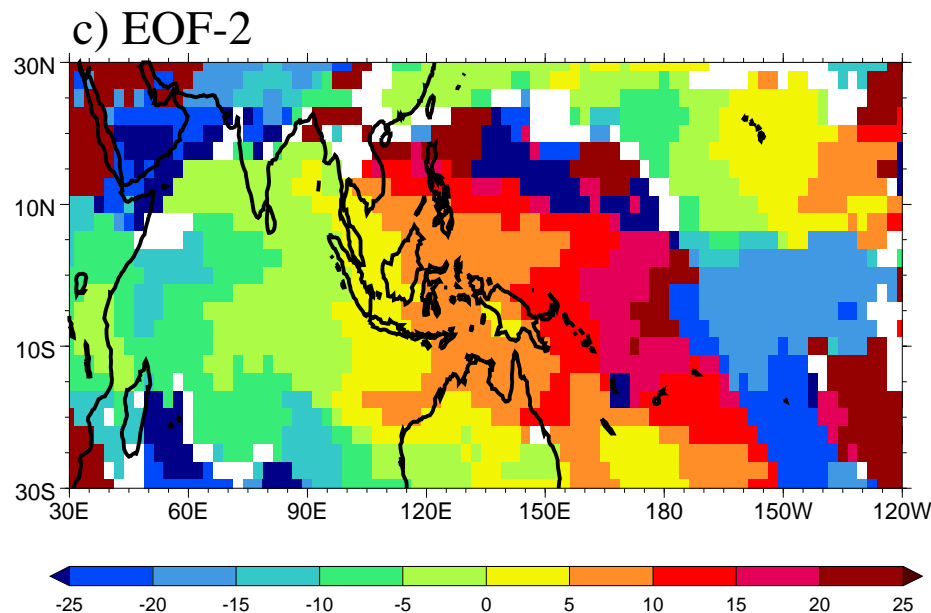
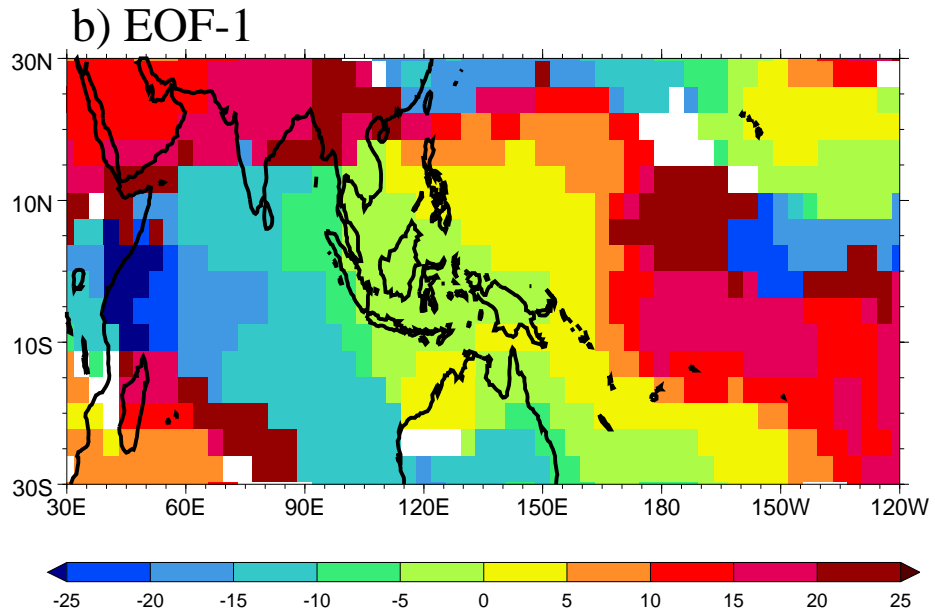


Day of maximum convection

AVHRR OLR

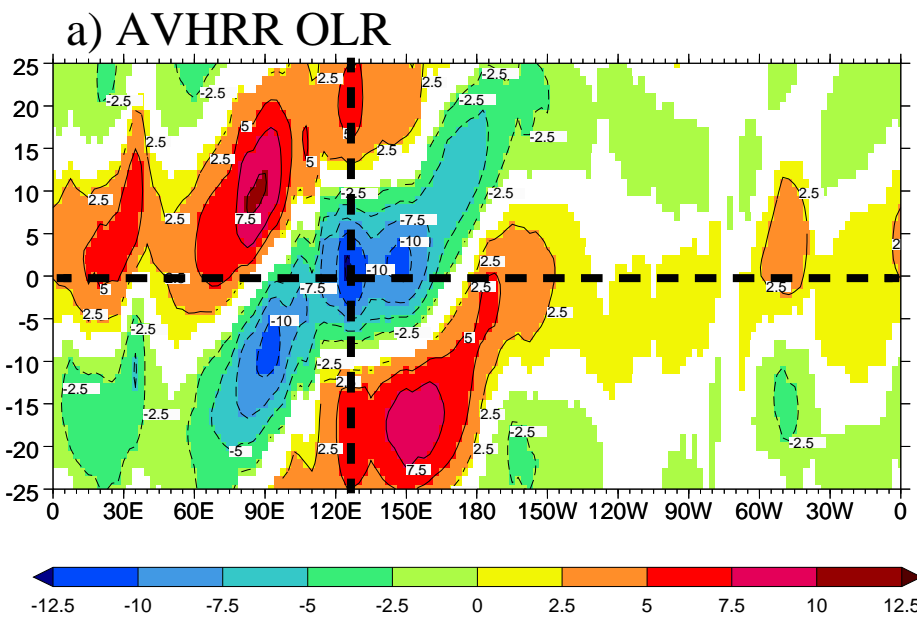


ECHAM4/HOPE

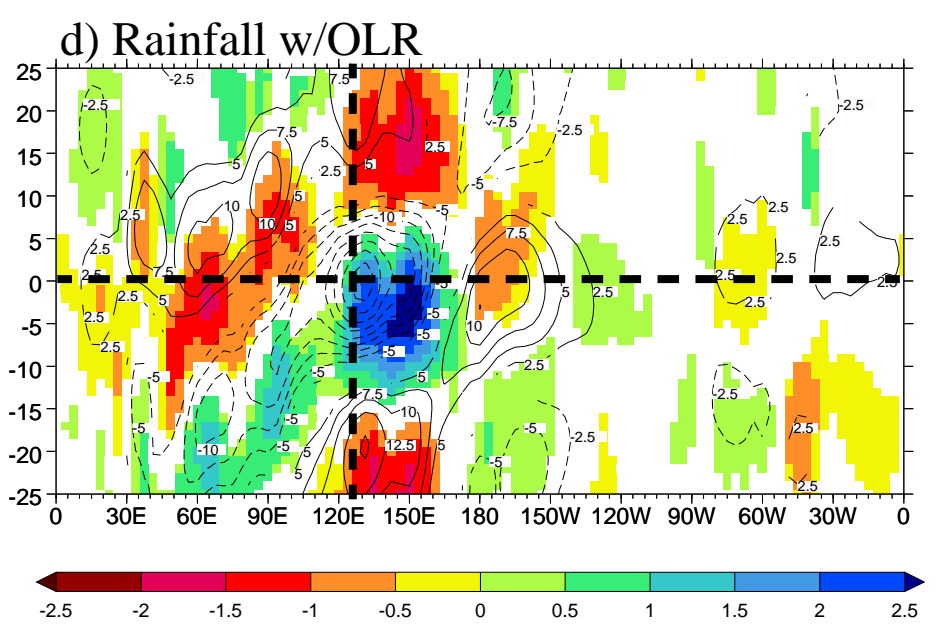
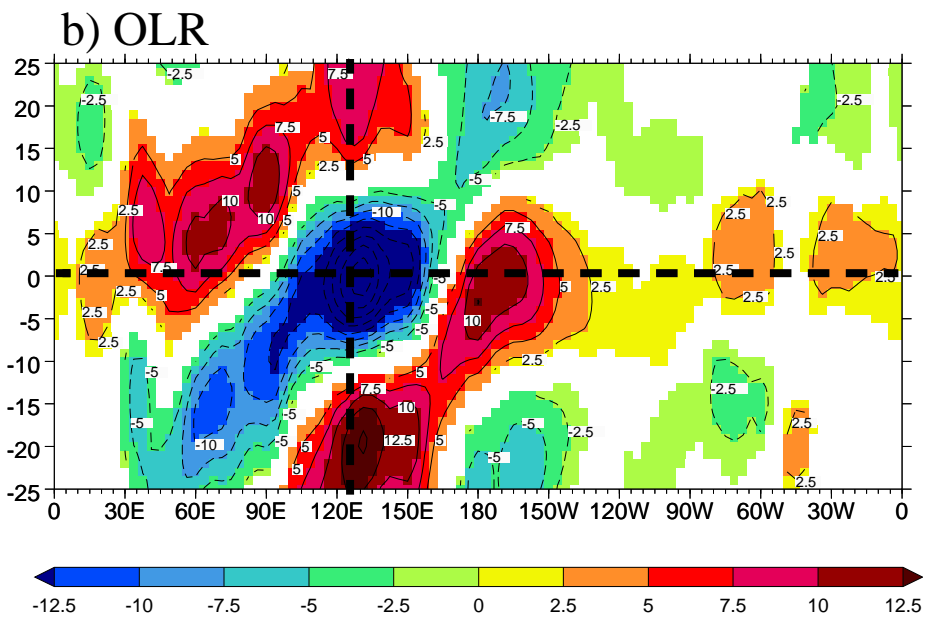


Lagged linear regression using PC-1 (5°N - 5°S)

Observations



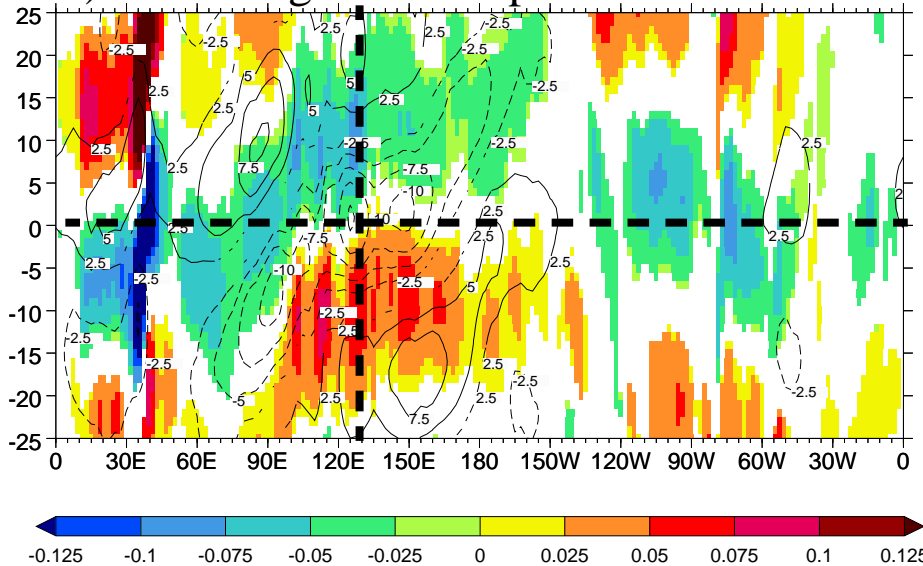
ECHAM4/HOPE



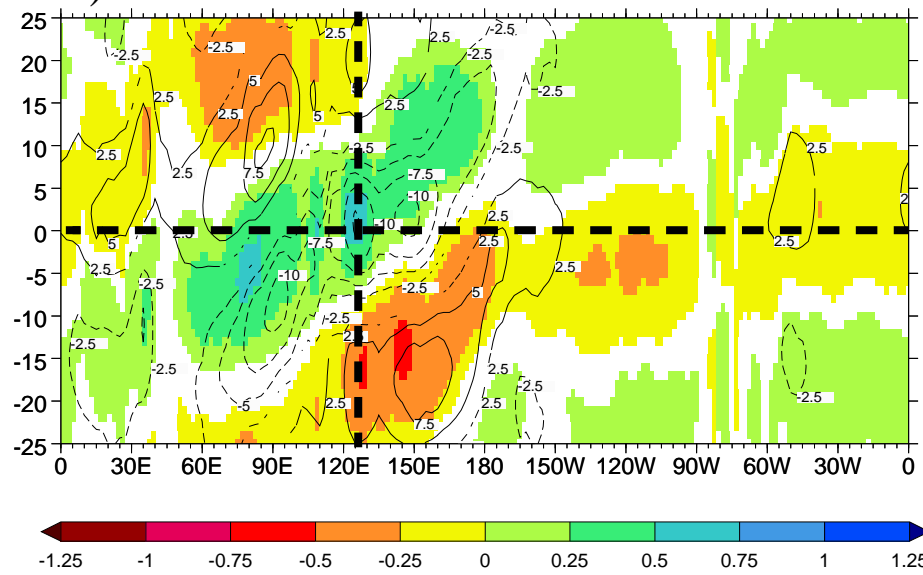
Lagged linear regression using PC-1 (5°N - 5°S)

Observations and NCEP/NCAR Reanalysis

a) SST and ground temperature w/OLR

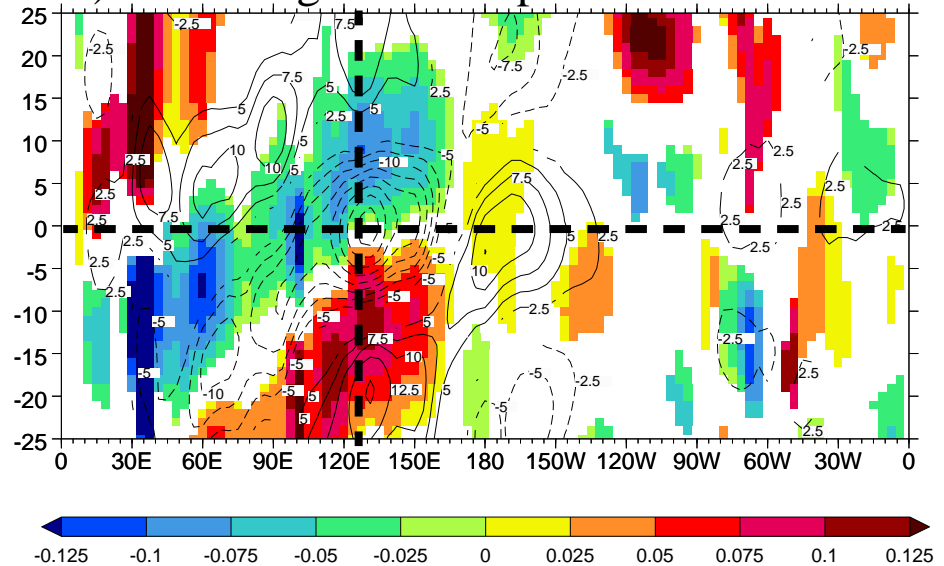


c) Surface zonal wind w/OLR

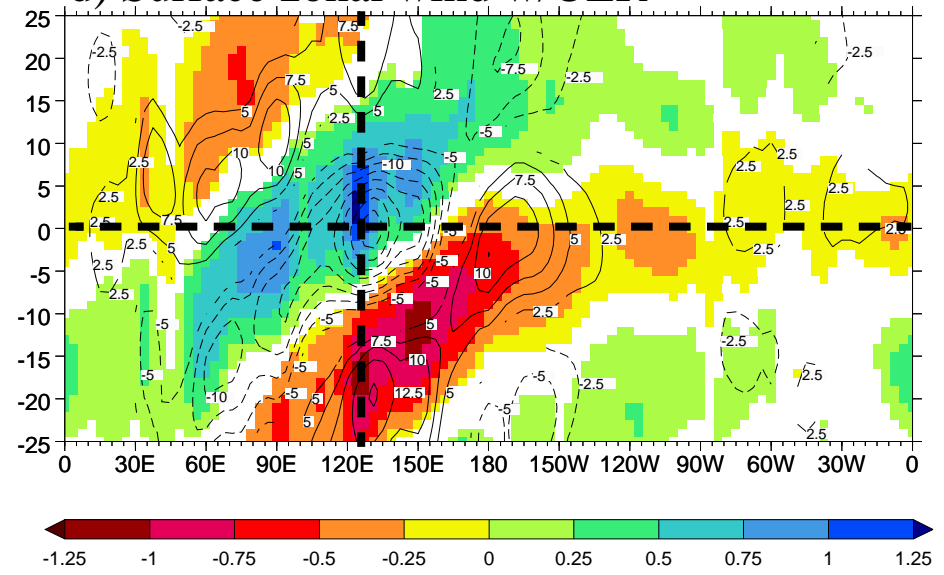


ECHAM4/HOPE

b) SST and ground temperature w/OLR



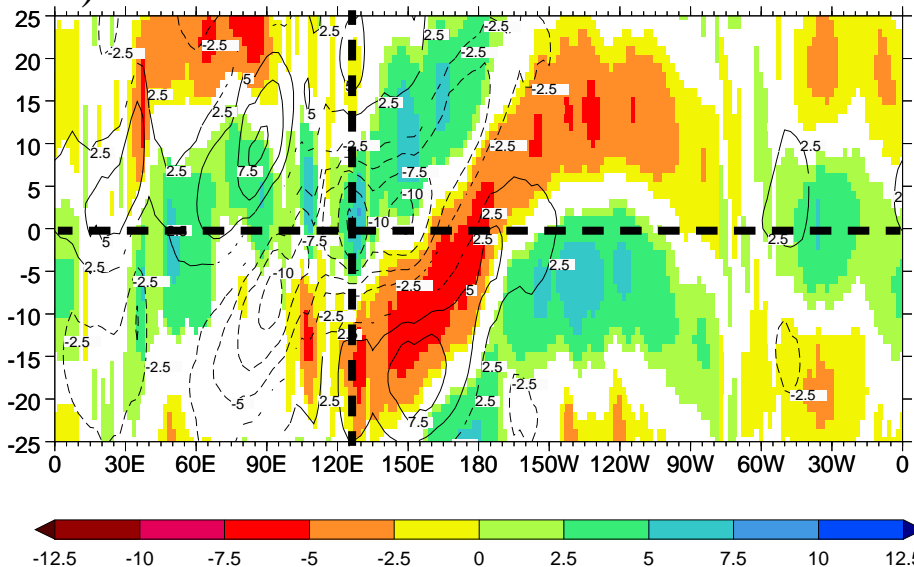
d) Surface zonal wind w/OLR



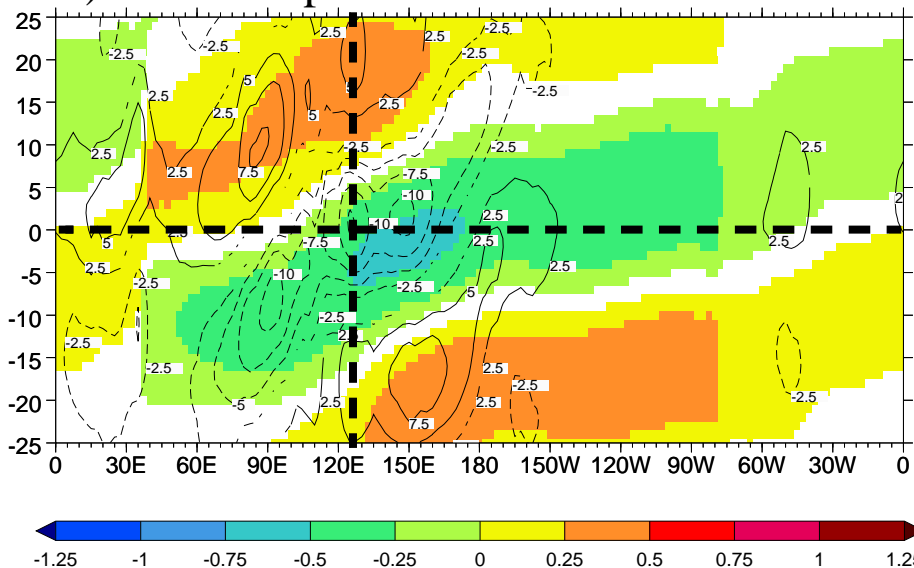
Lagged linear regression using PC-1 (5°N - 5°S)

Observations and NCEP/NCAR Reanalysis

a) Latent heat flux w/OLR

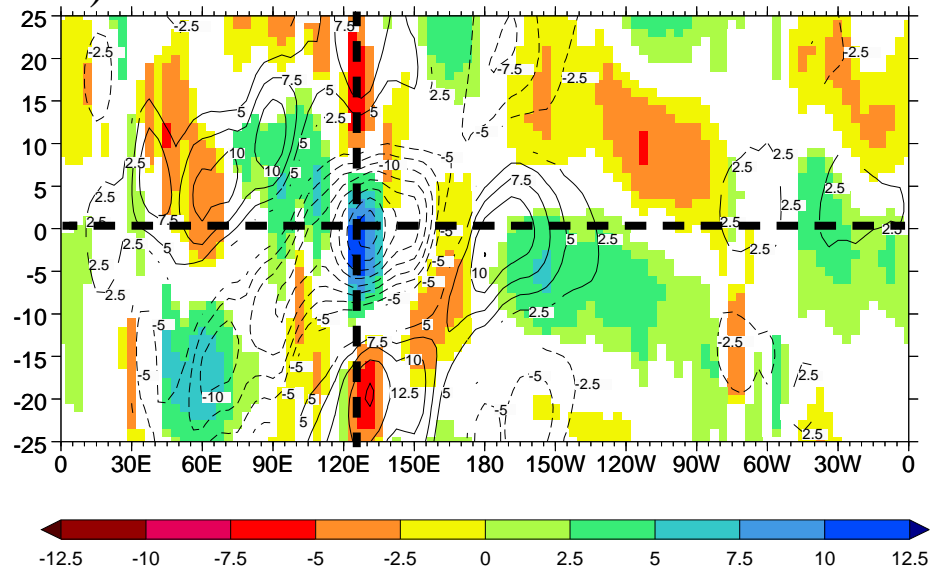


c) Sea-level pressure w/OLR

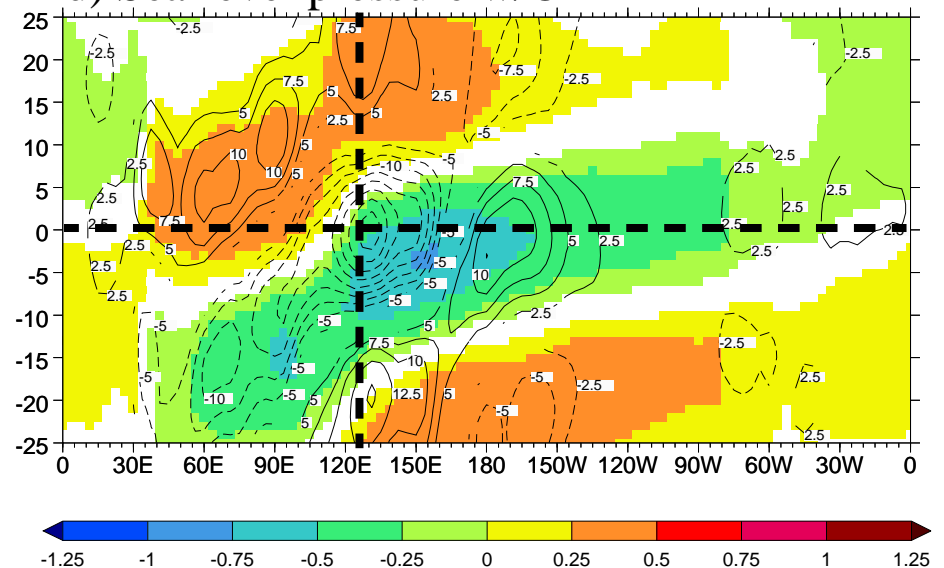


ECHAM4/HOPE

b) Latent heat flux w/OLR



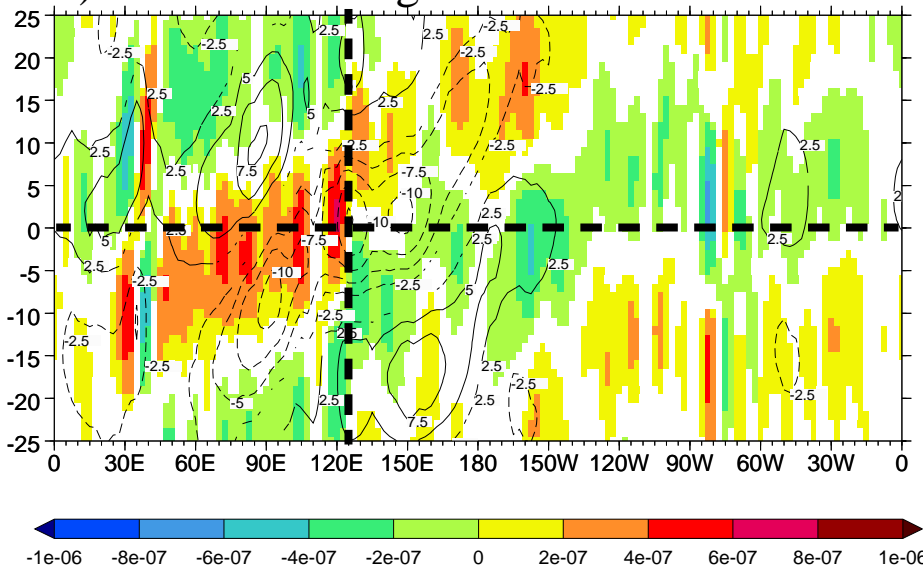
d) Sea-level pressure w/OLR



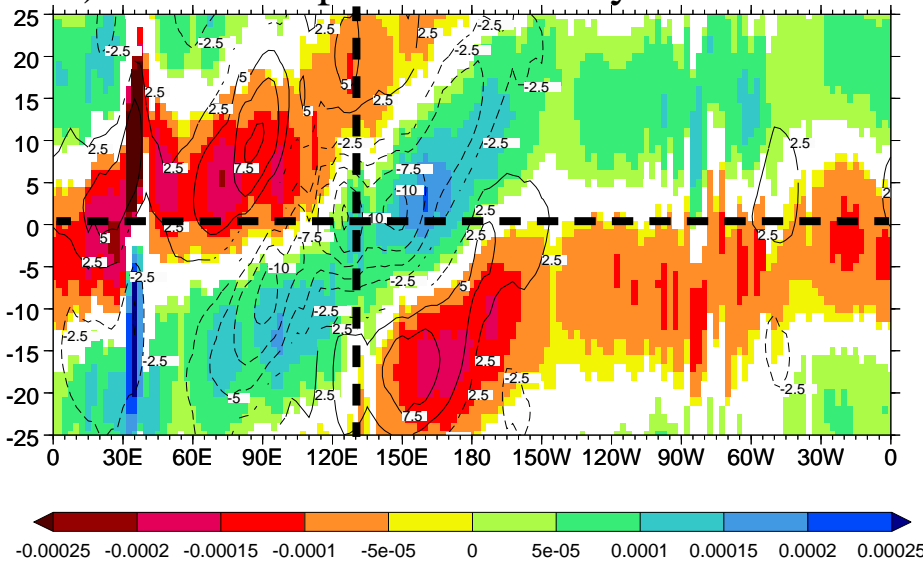
Lagged linear regression using PC-1 (5°N - 5°S)

Observations and NCEP/NCAR Reanalysis

a) 1000hPa Divergence w/OLR

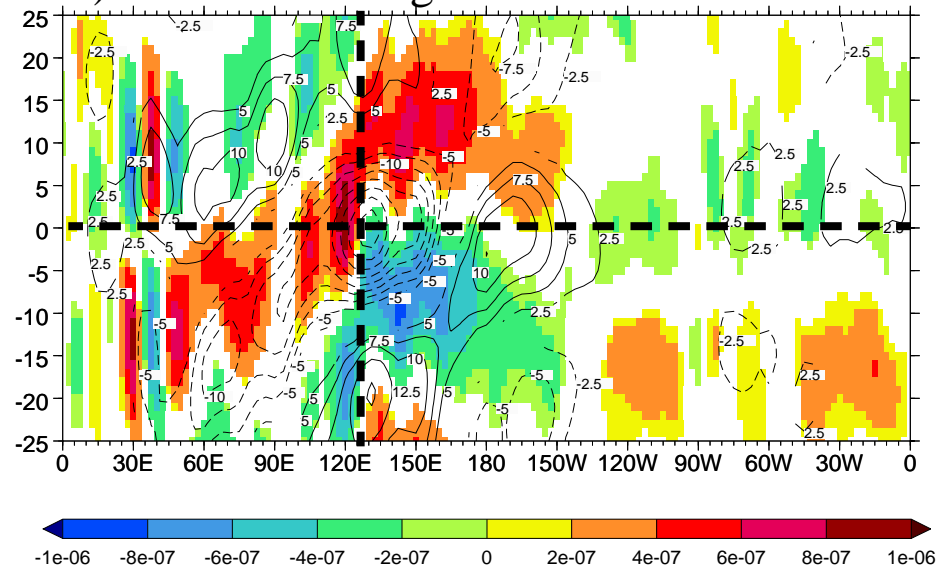


c) 1000hPa Specific humidity w/OLR

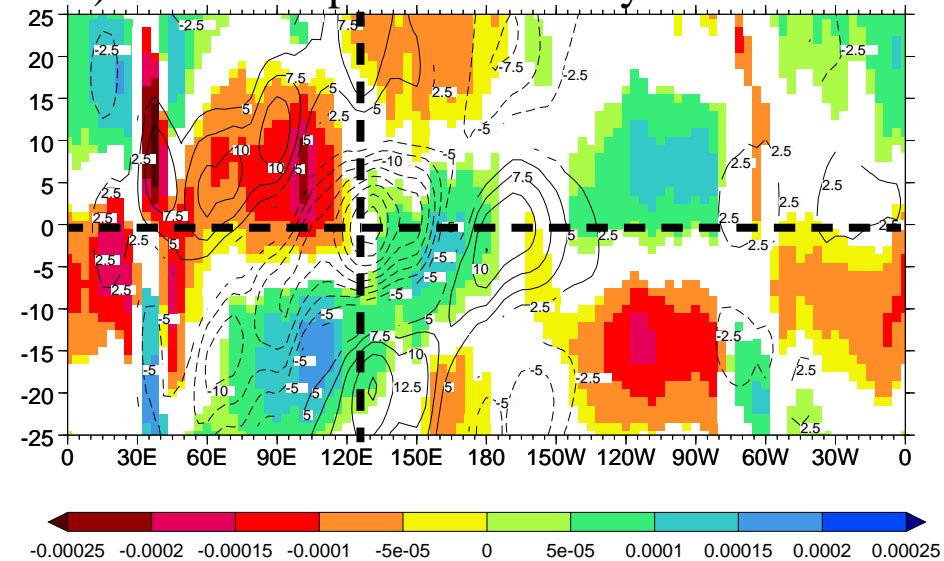


ECHAM4/HOPE

b) 1000hPa Divergence w/OLR



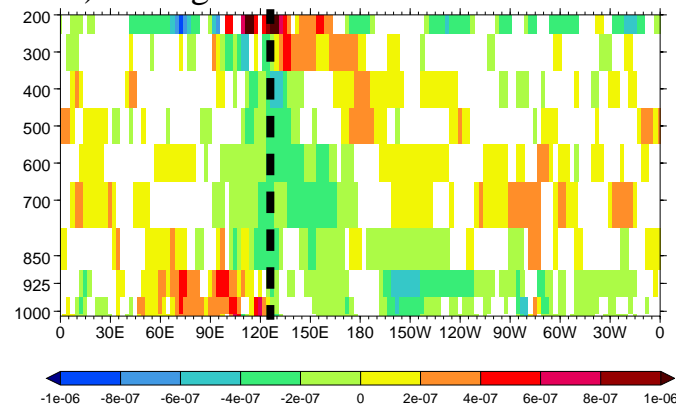
d) 1000hPa Specific humidity w/OLR



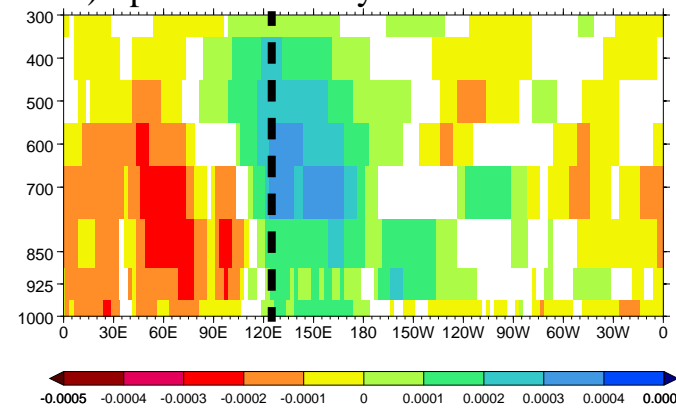
Lag 0 linear regression using PC-1 (5°N - 5°S)

NCEP/NCAR Reanalysis

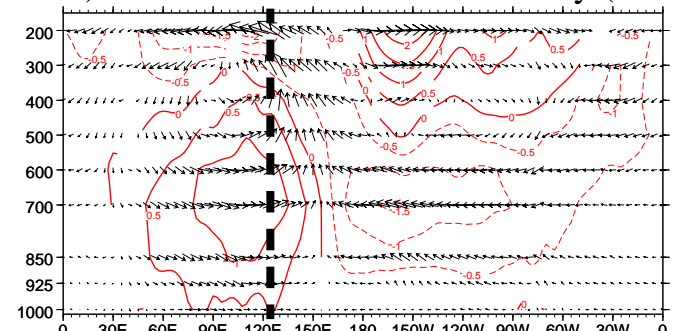
a) Divergence



c) Specific humidity



e) Zonal wind and vertical velocity (-100x)

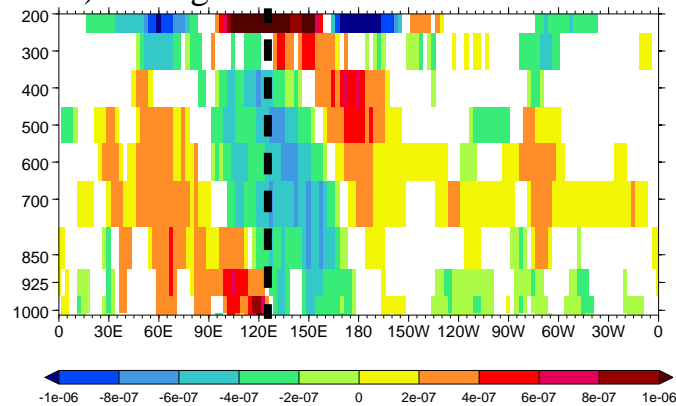


→

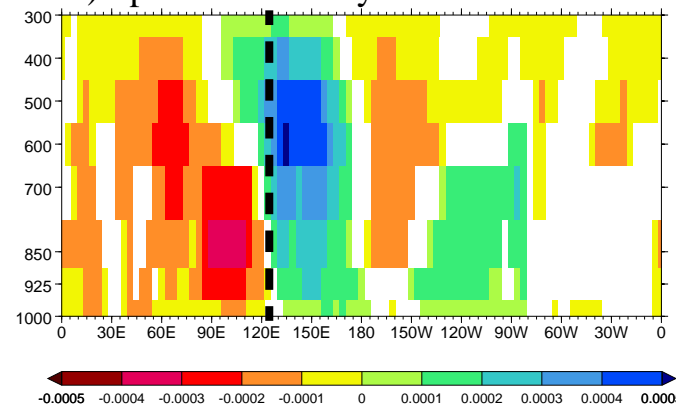
1

ECHAM4/HOPE

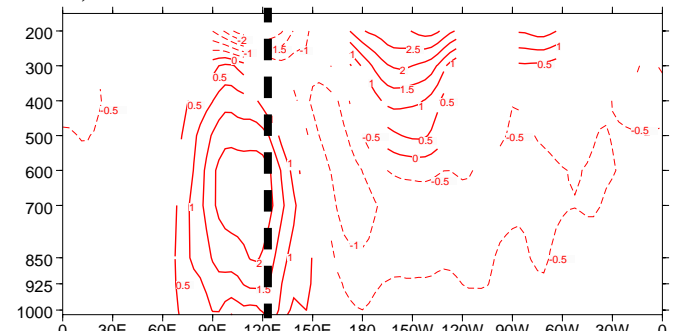
b) Divergence



d) Specific humidity

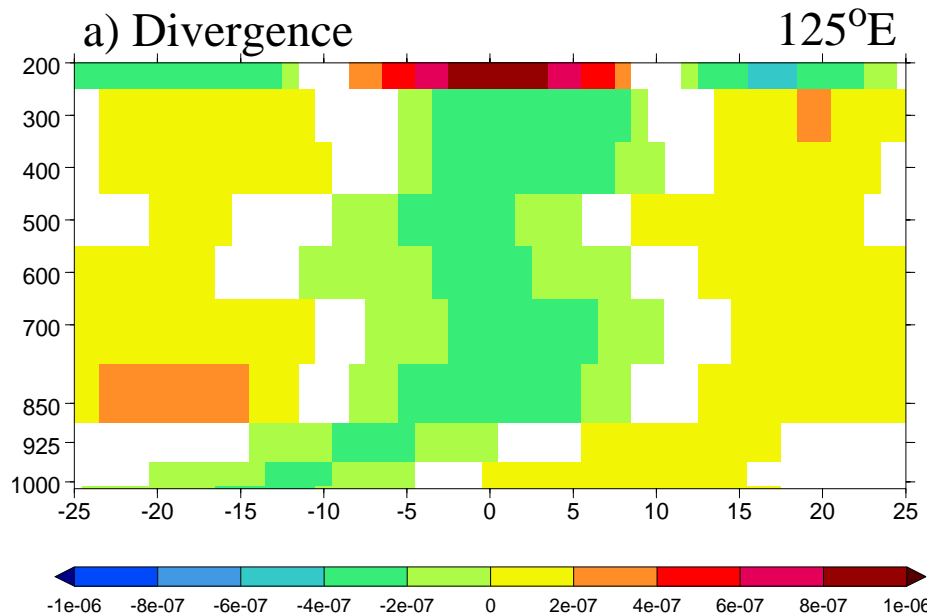


f) Zonal wind



Lagged linear regression using PC-1 (5°N - 5°S)

NCEP/NCAR Reanalysis



ECHAM4/HOPE

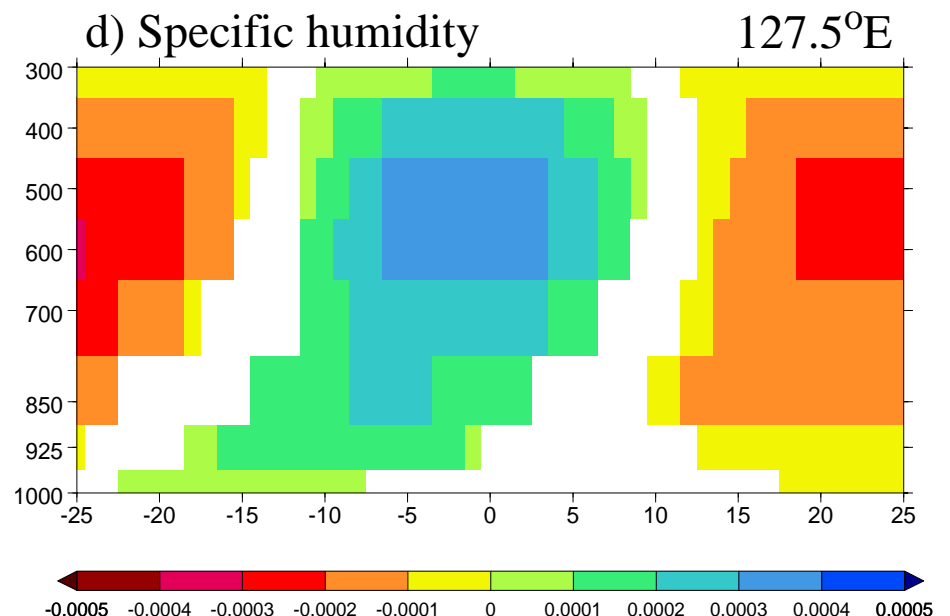
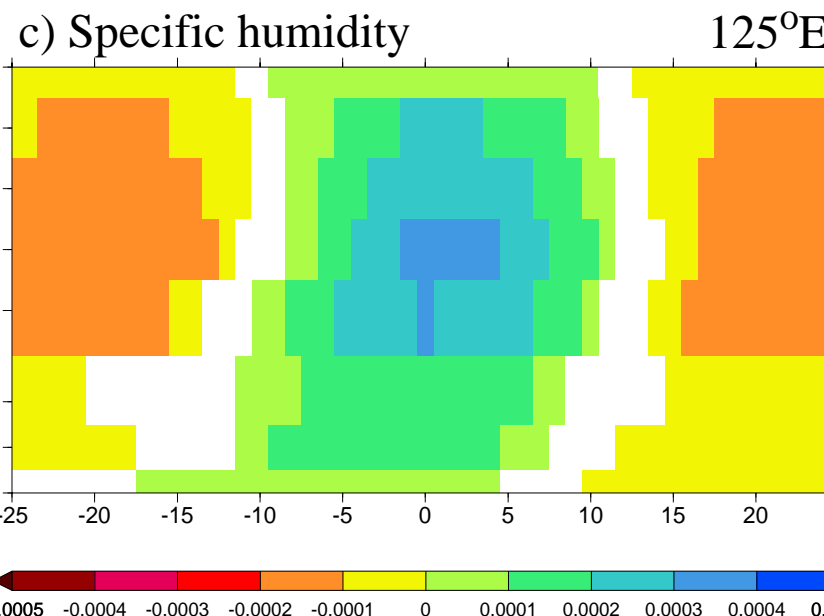
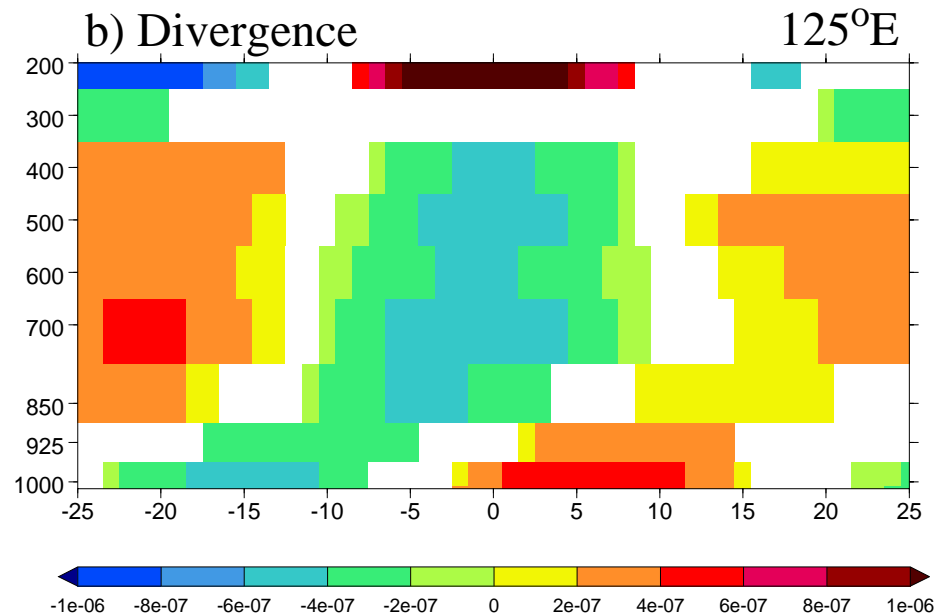


Table 1: Observed, reanalyzed, and AMIP Model MJO-eastward characteristics. Given are the standard deviations of PC-1 and PC-2, the maximum positive correlation, R, the time lag (days) at which it occurred, and the fraction of years for which the PC's had a lead-lag relationship consistent with the observations. Shaded models used the same atmospheric component in their coupled integration (see Table 2).

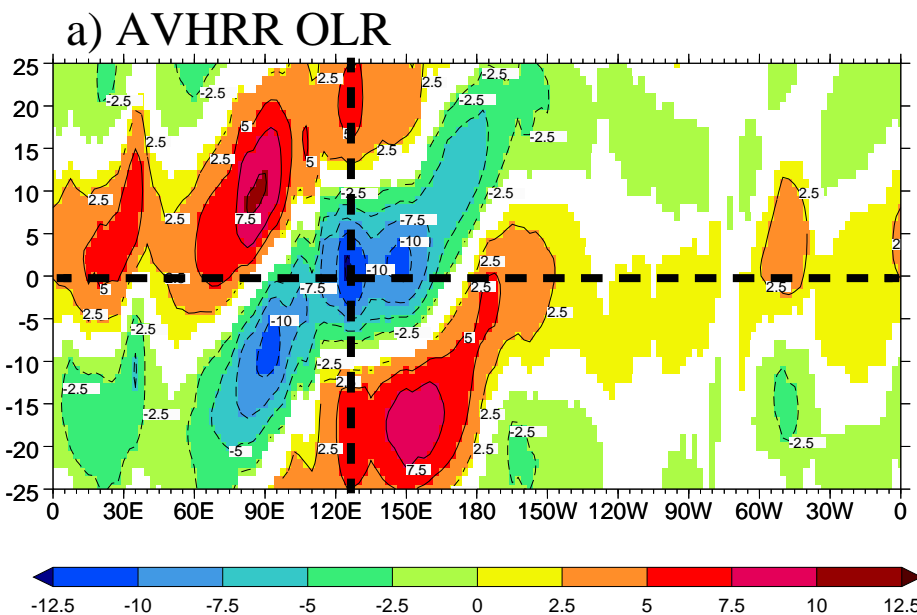
Model	PC-1	PC-2	R	Lag (days) PC-2 leads PC-1 (positive)	#Years Eastward/ Total
AVHRR	211.3	205.6	0.67	12	16/16
NCEP/NCAR	119.4	103.4	0.60	12	14/16
CCCMA	105.8	102.3	0.41	12	8/16
CCSR	109.7	91.0	0.41	12	10/16
CNRM	161.8	141.1	0.57	14	12/16
COLA	104.0	77.9	0.30	25	7/16
DNM	73.7	70.3	0.42	17	5/16
ECHAM4	221.2	232.2	0.43	12	11/16
ECMWF (T63)	100.7	97.5	0.42	19	4/16
ECMWF (T159)	130.8	84.8	0.58	21	4/16
GFDL	107.1	79.7	0.28	14	6/16
GFDL/DERF	158.4	186.4	0.41	12	13/16
GISS (A170)	36.2	36.2	0.27	20	3/16
GISS (Model II)	58.8	59.2	0.54	22	1/16
HADAM3 (L58)	125.4	99.0	0.42	13	9/16
HADAM2 (AMIP I)	182.6	137.9	0.48	18	6/9
JMA	165.0	159.3	0.35	10	10/16
MRI	185.0	159.6	0.46	9	7/16
NCAR CAM2	93.8	97.2	0.17	25	6/16
NCAR CCM3	83.7	82.8	0.37	16	7/16
NCEP (T42)	111.0	103.1	0.46	11	8/16
NCEP (T62)	102.7	96.1	0.41	21	7/16

Table 2: Observed, reanalyzed, and coupled model MJO-eastward characteristics. Given are the standard deviations of PC-1 and PC-2, the maximum positive correlation, R, the time lag (days) at which it occurred, and the fraction of years for which the PC's had a lead-lag relationship consistent with the observations. Shaded models used the same atmospheric component in their AMIP integration (see Table 1).

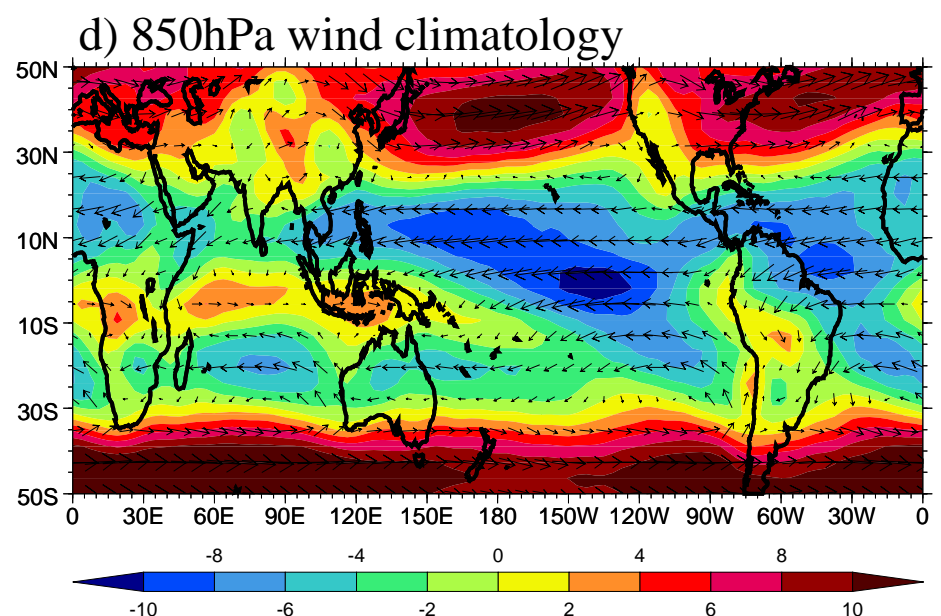
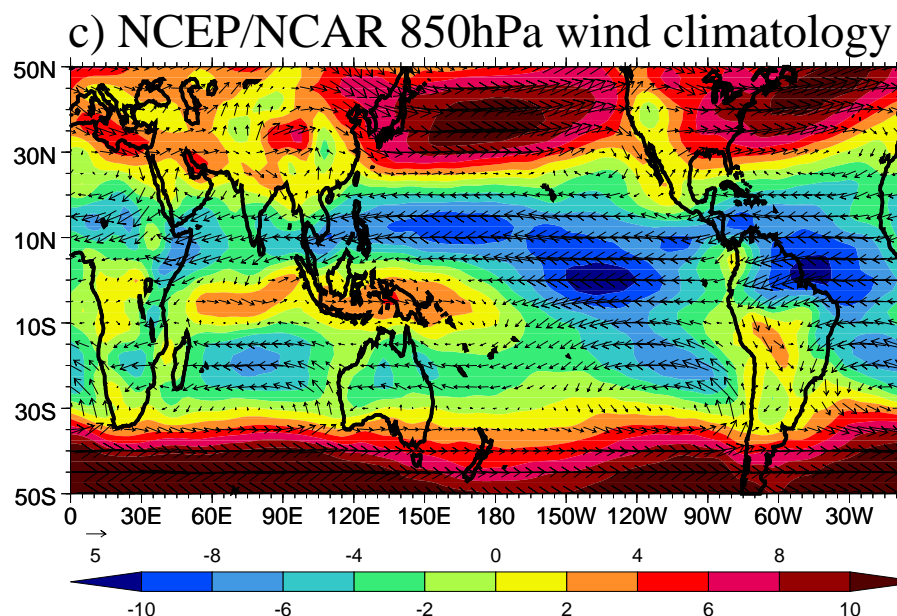
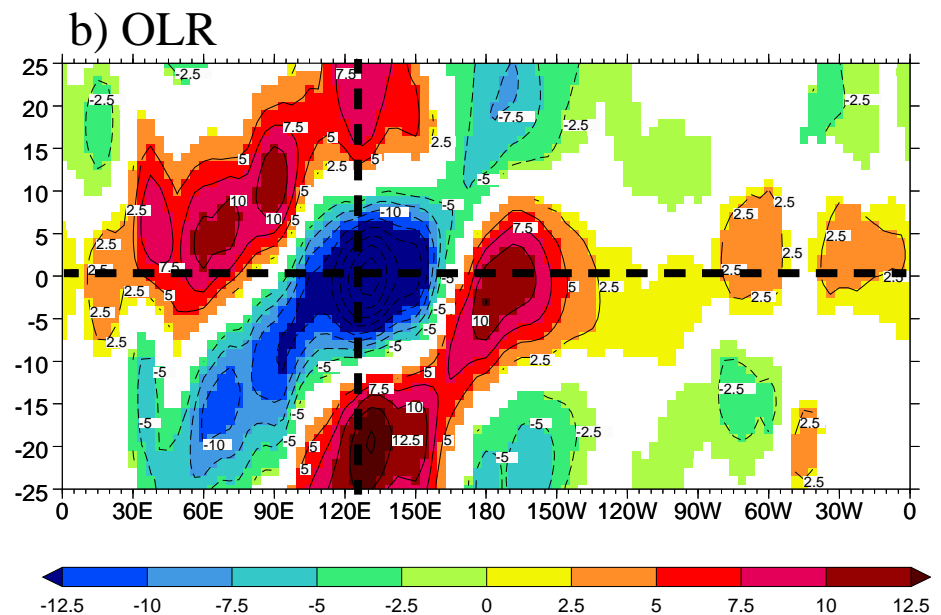
Model	PC-1	PC-2	R	Lag (days) PC-2 leads PC-1 (positive)	#Years Eastward/ Total
AVHRR	211.3	205.6	0.67	12	16/16
NCEP/NCAR	119.4	103.4	0.60	12	14/16
CSIRO	143.6	165.7	0.49	16	13/19
ECHAM4.6/HOPE (ECHO-G)	293.8	267.1	0.68	12	16/19
ECHAM4/OPA8.1 (SINTEX)	240.8	207.6	0.50	12	15/19
ECHAM4/OPYC3	245.8	217.9	0.71	11	19/19
GFDL R30	221.4	198.9	0.48	10	16/19
HADCM3 (L30)	105.5	99.8	0.51	8	14/19
IAP/LASG GOALS	127.4	132.8	0.47	10	7/9
NCAR CCSM2	103.6	119.8	0.40	16	5/9
NCAR PCM	109.4	94.9	0.42	15	10/15

MJO OLR propagation vs. the 850hPa wind climatology (Nov.-Mar.)

Observations (1979/80-1994/95)

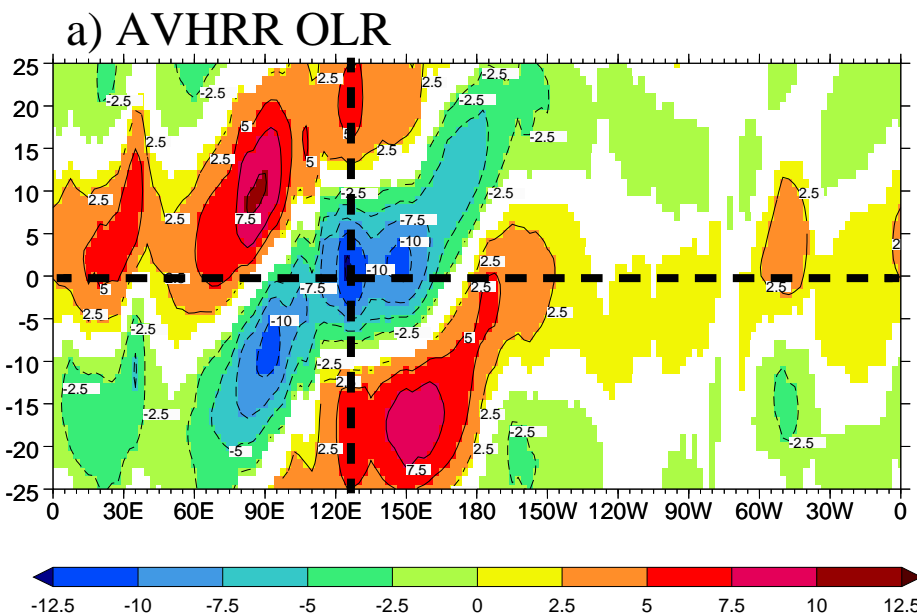


ECHAM4/HOPE

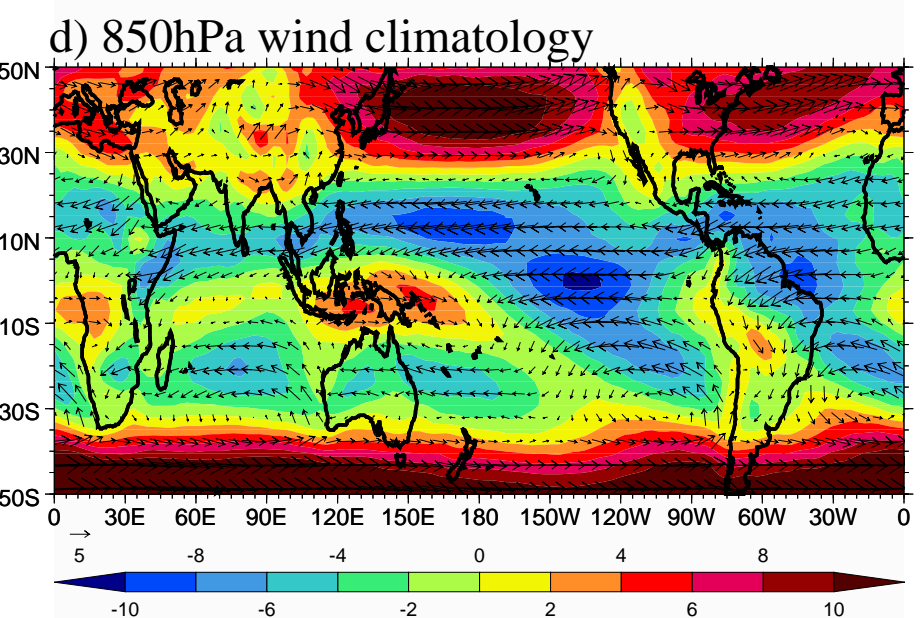
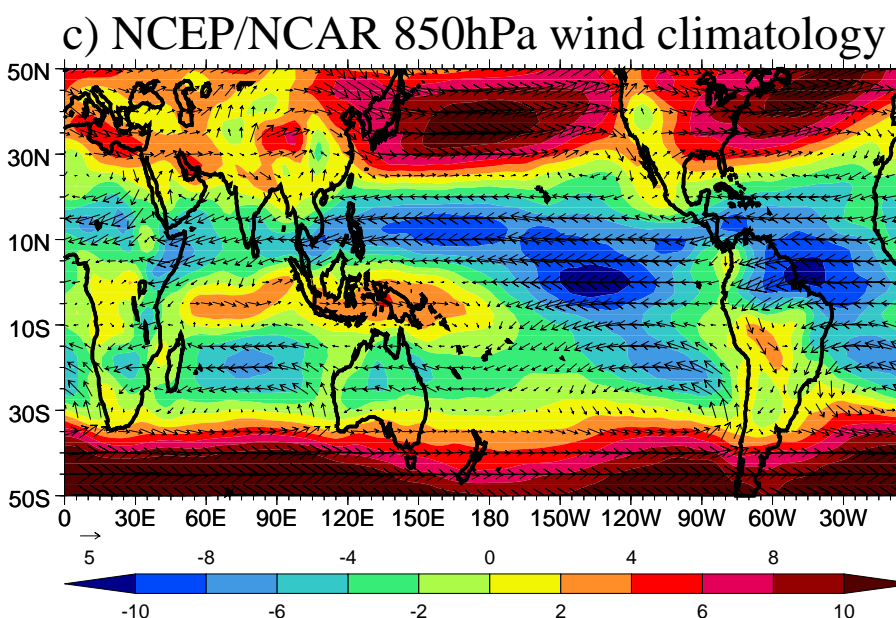
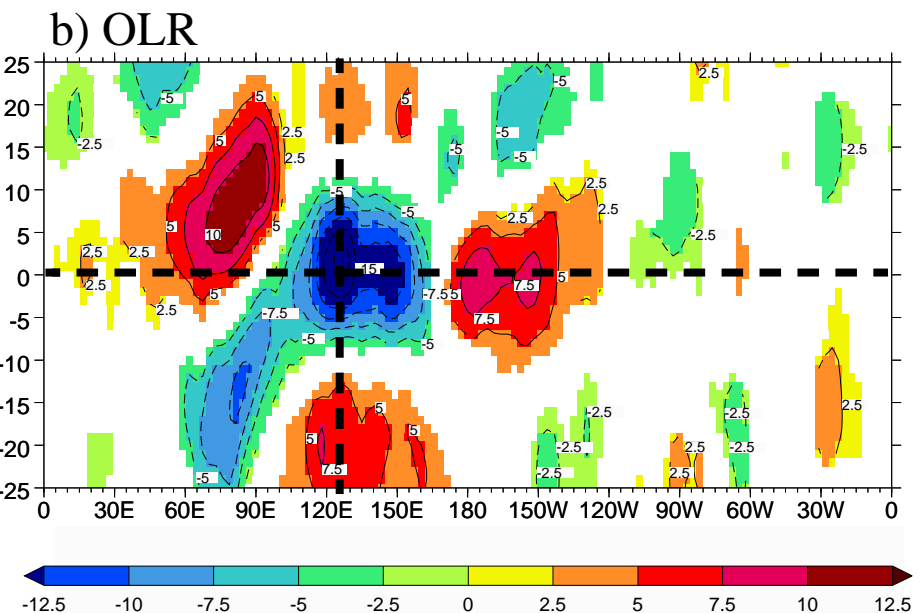


MJO OLR propagation vs. the 850hPa wind climatology (Nov.-Mar.)

Observations (1979/80-1994/95)

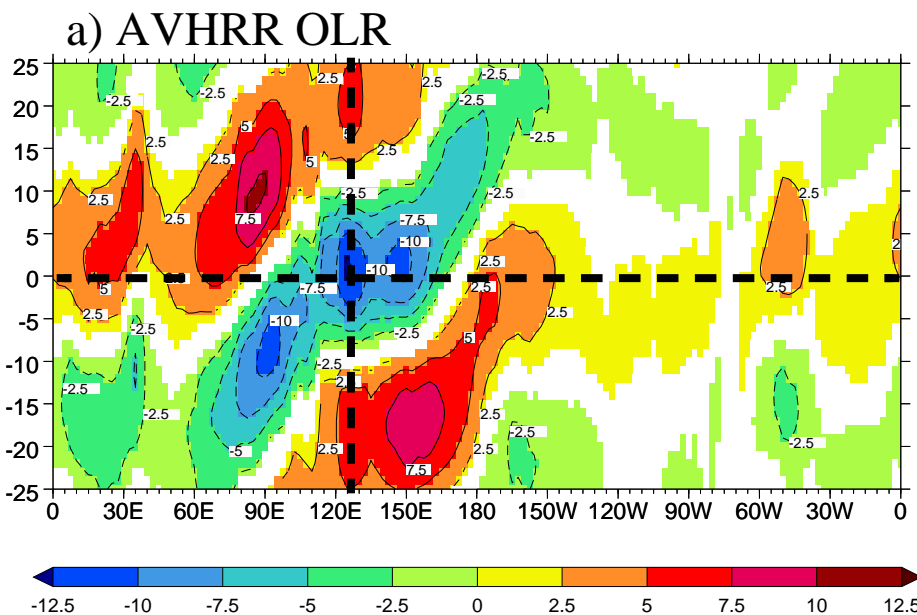


ECHAM4 (1979/80-1994/95)

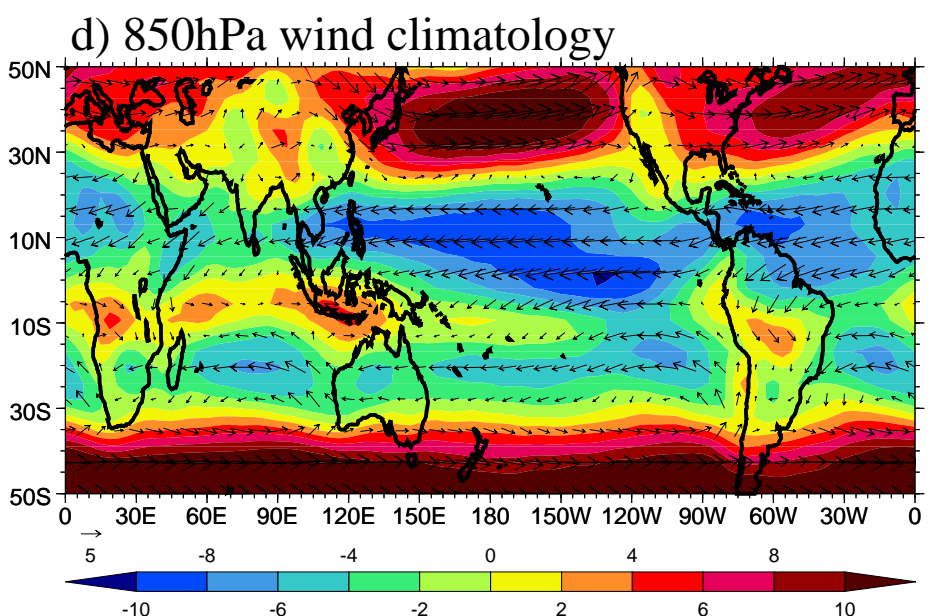
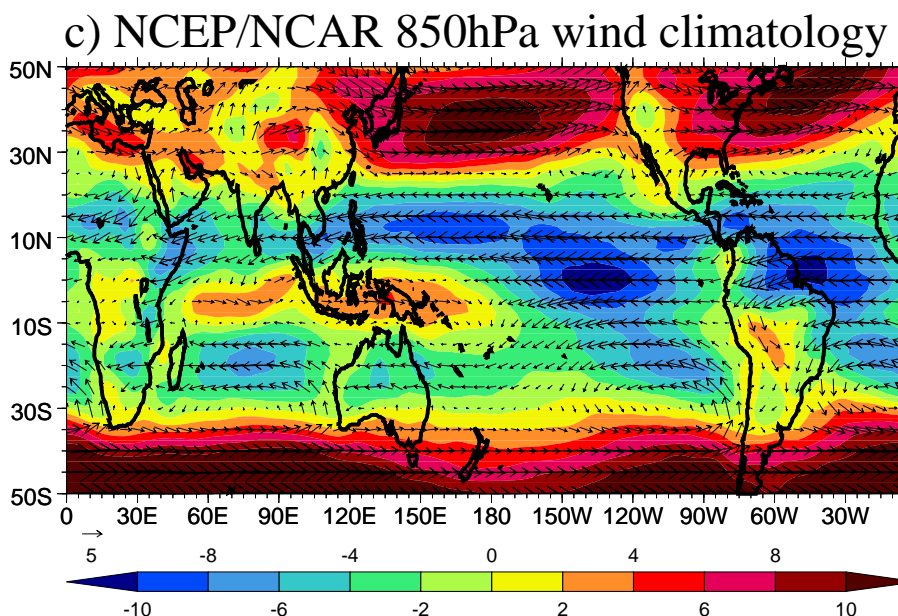
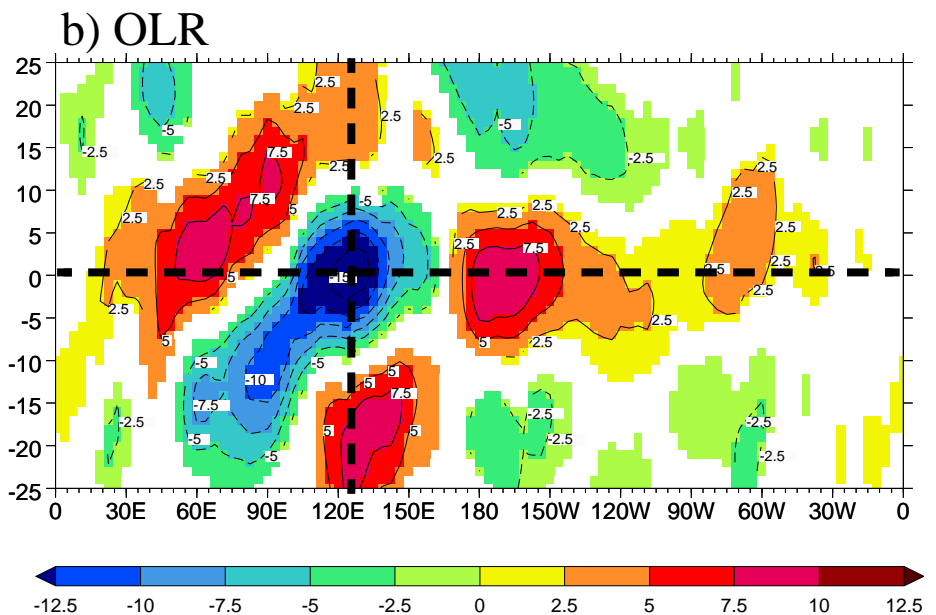


MJO OLR propagation vs. the 850hPa wind climatology (Nov.-Mar.)

Observations (1979/80-1994/95)

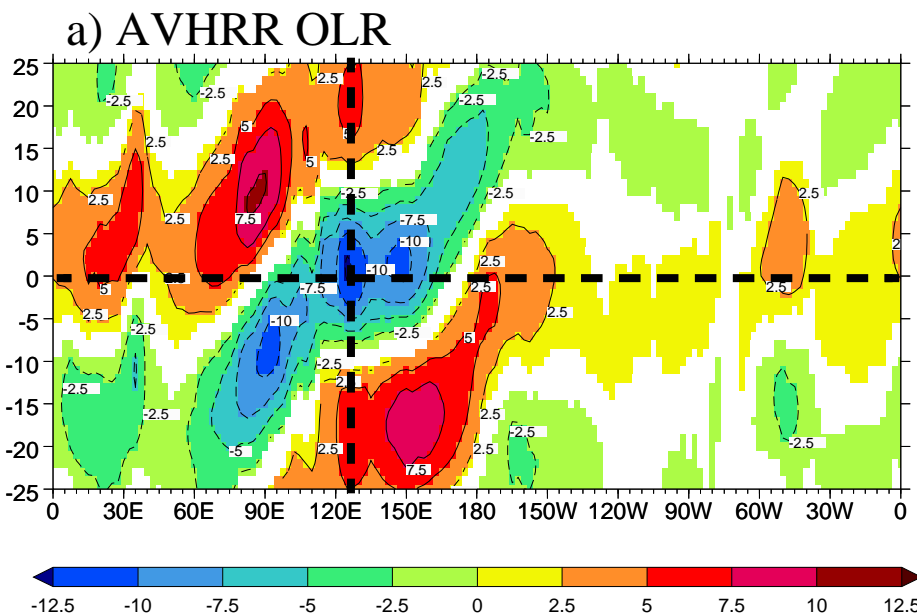


ECHAM4/OPA8.1

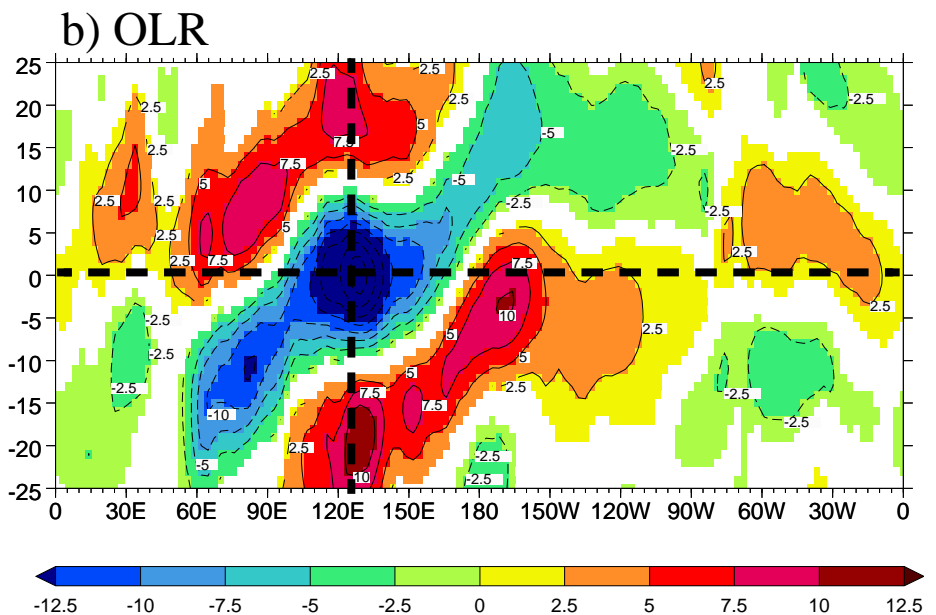


MJO OLR propagation vs. the 850hPa wind climatology (Nov.-Mar.)

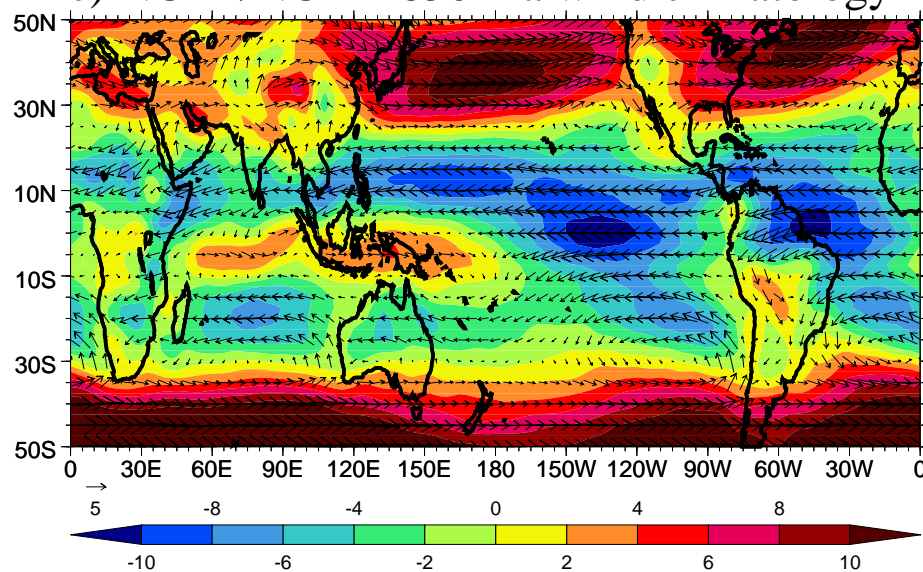
Observations (1979/80-1994/95)



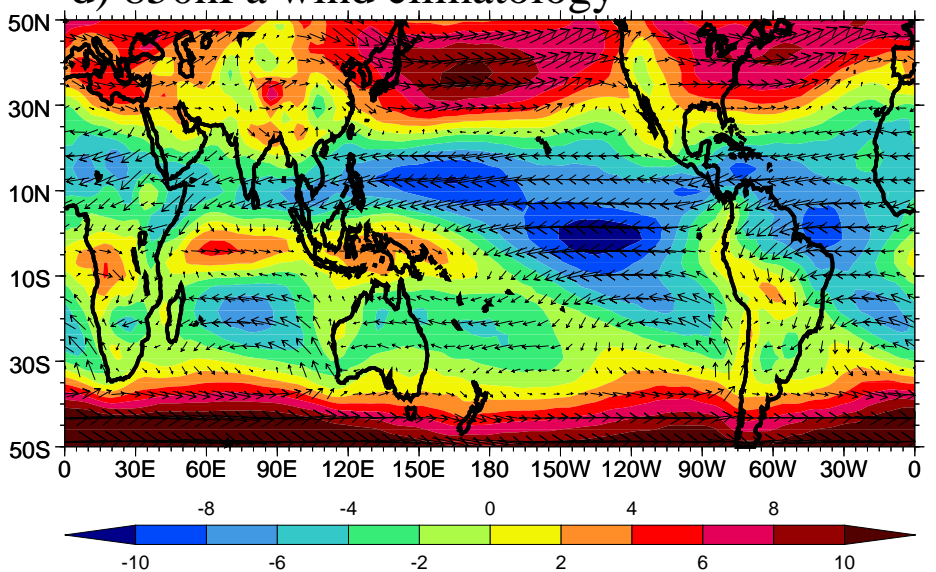
ECHAM4/OPYC



c) NCEP/NCAR 850hPa wind climatology



d) 850hPa wind climatology



Results

- 1) The MJO is a very stringent test of a models ability to simulate tropical variability
- 2) The models still fail to represent the intraseasonal dominance of the large-scale circulation
- 3) Within a family of models, ocean-atmosphere coupling leads to an improved lead/lag structure of the MJO
- 4) The ECHAM family of models produces a realistic representation of the MJO, though some problems exist (e.g., latent heat flux relation to MJO convection, details of the vertical structure)

Results (con't)

- 5) The propagation of convection into the western/central Pacific tends to be limited by systematic error of the lower-tropospheric zonal wind (e.g., eastward propagation impeded in presence of easterly winds)
- 6) For the other models a more comprehensive diagnosis of the MJO mechanism will require daily data:
 - latent heat flux
 - winds (standard pressure levels)
 - vertical velocity (standard pressure levels)
 - specific humidity (standard pressure levels)
 - diabatic heating profiles (pressure or model levels?)